ELSEVIER

Finite Elements in Analysis and Design 19 (1995) 169–179

FINITE ELEMENTS IN ANALYSIS AND DESIGN

Buckling analyses of fiber-composite laminate plates with material nonlinearity

Hsuan-Teh Hu

Department of Civil Engineering, National Cheng Kung University, Tainan, Taiwan 70101, ROC

Abstract

A nonlinear material constitutive model, including a nonlinear in-plane shear formulation and a failure criterion, for fiber-composite laminate materials is employed to carry out finite element buckling analyses for composite plates under uniaxial compressive loads. It has been shown that the nonlinear in-plane shear together with the failure criterion have significant influence on the buckling behavior of composite laminate plates.

1. Introduction

The use of fiber reinforced composite laminate plates in aerospace structures has increased rapidly in recent years. The composite plate structures are commonly subjected to various kinds of compression which may cause buckling. Therefore, knowledge of the buckling and postbuckling behavior of composite plates has become essential in design. In the literature, most stability studies of composite laminate plates have been limited to the geometrically nonlinear analysis [1–4]. Little attention has been paid to the material nonlinearity.

It is well known that unidirectional fibrous composites exhibit severe nonlinearity in in-plane shear stress–strain relation. In addition, deviation from linearity is also observed in transverse loading but the degree of nonlinearity is not comparable to that in the in-plane shear [5]. For graphite/epoxy and boron/epoxy, this nonlinearity associated with the transverse loading can usually be ignored [6].

A significant number of macromechanical models have been proposed to represent the constitutive relation of fiber-composite materials such as nonlinear elasticity models [5, 7, 8], or plasticity models [9–12]. In addition, various failure criteria have also been proposed to predict the onset of failure in single layer of fiber-reinforced composites, such as maximum strain theory, maximum stress theory, Tsai–Wu theory, Hoffman theory, etc. [13]. The mechanical response of fiber-composite materials is very complicated. Since the nonlinearity of in-plane shear is significant for composite materials, this work is therefore focusing on the influence of the

0168-874X/95/$09.50
SSDI 0168-874X(95)00009-7

in-plane shear nonlinearity together with a failure criterion on the buckling response of composite plates.

In this paper, a material model including the nonlinear in-plane shear and the Tsai–Wu failure criterion is reviewed first. Then, nonlinear buckling analyses for simply supported composite plates under uniaxial compression are carried out using the ABAQUS finite element program [14]. Numerical results for the material nonlinear buckling behavior of these composite plates are compared with those using linear material properties. Finally, important conclusions obtained from this study are given.

2. Constitutive modeling of lamina

For fiber-composite laminate materials, each lamina can be considered as an orthotropic layer in a plane stress condition. The incremental stress–strain relations for a linear orthotropic lamina in the material coordinates (1, 2, 3) can be written as

$$\Delta\{\sigma'\} = [Q_1']\Delta\{\varepsilon'\}, \tag{1}$$

$$\Delta\{\tau_t'\} = [Q_2']\Delta\{\gamma_t'\}, \tag{2}$$

where $\Delta\{\sigma'\} = \Delta\{\sigma_1, \sigma_2, \tau_{12}\}^T$, $\Delta\{\tau_t'\} = \Delta\{\tau_{13}, \tau_{23}\}^T$, $\Delta\{\varepsilon'\} = \Delta\{\varepsilon_1, \varepsilon_2, \gamma_{12}\}^T$, $\Delta\{\gamma_t'\} = \Delta\{\gamma_{13}, \gamma_{23}\}^T$, and

$$[Q_1'] = \begin{bmatrix} \dfrac{E_{11}}{1 - \nu_{12}\nu_{21}} & \dfrac{\nu_{12}E_{22}}{1 - \nu_{12}\nu_{21}} & 0 \\ \dfrac{\nu_{21}E_{11}}{1 - \nu_{12}\nu_{21}} & \dfrac{E_{22}}{1 - \nu_{12}\nu_{21}} & 0 \\ 0 & 0 & G_{12} \end{bmatrix}, \tag{3}$$

$$[Q_2'] = \begin{bmatrix} \alpha_1 G_{13} & 0 \\ 0 & \alpha_2 G_{23} \end{bmatrix}, \tag{4}$$

where α_1 and α_2 are the shear correction factors [15] and are taken to be 0.83 in this study.

To model the nonlinear in-plane shear behavior, the nonlinear strain–stress relation for a composite lamina suggested by Hahn and Tsai [5] is adopted in this study, which is given as follows:

$$\begin{Bmatrix} \varepsilon_1 \\ \varepsilon_2 \\ \gamma_{12} \end{Bmatrix} = \begin{bmatrix} \dfrac{1}{E_{11}} & -\dfrac{\nu_{21}}{E_{22}} & 0 \\ -\dfrac{\nu_{12}}{E_{11}} & \dfrac{1}{E_{22}} & 0 \\ 0 & 0 & \dfrac{1}{G_{12}} \end{bmatrix} \begin{Bmatrix} \sigma_1 \\ \sigma_2 \\ \tau_{12} \end{Bmatrix} + S_{6666}\tau_{12}^2 \begin{Bmatrix} 0 \\ 0 \\ \tau_{12} \end{Bmatrix}. \tag{5}$$

In this model only one constant S_{6666} is required to account for the in-plane shear nonlinearity. The value of S_{6666} can be determined by a curve fit to various off-axis tension test data [5]. Inverting and differentiating Eq. (5), we can obtain the nonlinear incremental constitutive matrix for the lamina as follows:

$$[Q_1'] = \begin{bmatrix} \dfrac{E_{11}}{1-\nu_{12}\nu_{21}} & \dfrac{\nu_{12}E_{22}}{1-\nu_{12}\nu_{21}} & 0 \\ \dfrac{\nu_{21}E_{11}}{1-\nu_{12}\nu_{21}} & \dfrac{E_{22}}{1-\nu_{12}\nu_{21}} & 0 \\ 0 & 0 & \dfrac{1}{1/G_{12}+3S_{6666}\tau_{12}^2} \end{bmatrix}. \tag{6}$$

The validity of using Eq. (6) to model the nonlinear in-plane shear has been demonstrated by the paper of Hahn and Tsai [5] and is not repeated here. Furthermore, it is assumed that the transverse shear stresses always behave linearly and do not affect the nonlinear behavior of in-plane shear. Hence, the same shear correction factors and shear moduli for transverse shear as those given in Eq. (4) also apply to the cases of nonlinear in-plane shear.

3. Failure criterion and degradation of stiffness

Among existing failure criteria, the Tsai–Wu criterion [16] has been extensively used in literature and it is adopted in this analysis. Under plane stress conditions, this failure criterion has the following form:

$$F_1\sigma_1 + F_2\sigma_2 + F_{11}\sigma_1^2 + 2F_{12}\sigma_1\sigma_2 + F_{22}\sigma_2^2 + F_{66}\sigma_{12}^2 = 1, \tag{7}$$

where

$$F_1 = \frac{1}{X} + \frac{1}{X'}, \qquad F_2 = \frac{1}{Y} + \frac{1}{Y'}, \qquad F_{11} = \frac{-1}{XX'}, \qquad F_{22} = \frac{-1}{YY'}, \qquad F_{66} = \frac{1}{S^2}.$$

The X, Y and X', Y' are the lamina longitudinal and transverse strengths in tension and compression, respectively, and S is the shear strength of the lamina. Though the stress interaction term F_{12} in Eq. (7) is difficult to be determined, it has been suggested by Narayanaswami and Adelman [17] that F_{12} can be set equal to zero for practical engineering applications. Therefore, $F_{12} = 0$ is used in this investigation.

During the numerical calculation, incremental loading is applied to composite plates until failure in one or more of individual plies is indicated according to Eq. (7). Since the Tsai–Wu criterion does not distinguish failure modes, the following two rules are used to determine whether the ply failure is caused by resin fracture or fiber breakage [13]:

(1) If a ply fails but the stress in the fiber direction remains less than the uniaxial strength of the lamina in the fiber direction, i.e. $X' < \sigma_1 < X$, the ply failure is assumed to be resin induced.

Consequently, the laminate loses its capability to support transverse and shear stresses, but remains to carry longitudinal stress. In this case, the constitute matrix of the lamina becomes

$$[Q_1'] = \begin{bmatrix} E_{11} & 0 & 0 \\ 0 & 0 & 0 \\ 0 & 0 & 0 \end{bmatrix}. \tag{8}$$

(2) If a ply fails with σ_1 exceeding the uniaxial strength of the lamina, the ply failure is caused by the fiber breakage and a total ply rupture is assumed. In this case, the constitutive matrix of the lamina becomes

$$[Q_1'] = \begin{bmatrix} 0 & 0 & 0 \\ 0 & 0 & 0 \\ 0 & 0 & 0 \end{bmatrix}. \tag{9}$$

4. Constitutive modeling of composite shell section

The elements used in the finite element analyses are eight-node isoparametric shell elements with six degrees of freedom per node (three displacements and three rotations). The formulation of the shell allows transverse shear deformation [14, 18] and these shear flexible shells can be used for both thick and thin shell analysis [14].

During a finite element analysis, the constitutive matrix of composite materials at the integration points of shell elements must be calculated before the stiffness matrices are assembled from the element level to the structural level. For composite materials, the incremental constitutive equations of a lamina in the element coordinates (x, y, z) can be written as

$$\Delta\{\sigma\} = [Q_1]\Delta\{\varepsilon\}, \tag{10}$$

$$\Delta\{\tau_1\} = [Q_2]\Delta\{\gamma_t\}, \tag{11}$$

where $\Delta\{\sigma\} = \Delta\{\sigma_x, \sigma_y, \tau_{xy}\}^T$, $\Delta\{\tau_t\} = \Delta\{\tau_{xz}, \tau_{yz}\}^T$, $\Delta\{\varepsilon\} = \Delta\{\varepsilon_x, \varepsilon_y, \gamma_{xy}\}^T$, $\Delta\{\gamma_t\} = \Delta\{\gamma_{xz}, \gamma_{yz}\}^T$,

$$[Q_1] = [T_1]^T[Q_1'][T_1], \tag{12}$$

$$[Q_2] = [T_2]^T[Q_2'][T_2], \tag{13}$$

$$[T_1] = \begin{bmatrix} \cos^2\theta & \sin^2\theta & \sin\theta\cos\theta \\ \sin^2\theta & \cos^2\theta & -\sin\theta\cos\theta \\ -2\sin\theta\cos\theta & 2\sin\theta\cos\theta & \cos^2\theta - \sin^2\theta \end{bmatrix}, \tag{14}$$

$$[T_2] = \begin{bmatrix} \cos\theta & \sin\theta \\ -\sin\theta & \cos\theta \end{bmatrix} \tag{15}$$

and θ is measured counterclockwise from the element local x-axis to the material 1-axis (Fig. 1).

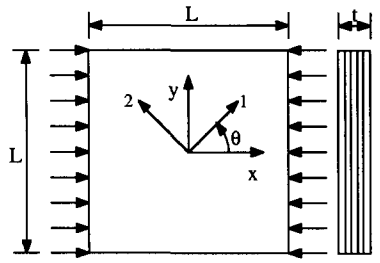

Laminate layups:
$[90/0]_{2S}$
$[45/-45]_{2S}$

Plate geometry:
L = 10.16 cm (4 in.)
t = 0.81cm (0.32 in.)

Ply constitutive properties:
E_{11} = 138 GPa
E_{22} = 14.5 GPa
$G_{12} = G_{13}$ = 5.86 GPa
G_{23} = 3.52 GPa
ν_{12} = 0.21
S_{6666} = 7.31 $(GPa)^{-3}$

Ply strengths:
X = 1450 MPa
X' = -1450 MPa
Y = 52 MPa
Y' = -206 MPa
S = 93 MPa

Fig. 1. Geometric and material properties for graphite/epoxy composite laminate plate.

Assume $\Delta\{\varepsilon_0\} = \Delta\{\varepsilon_{x0}, \varepsilon_{y0}, \gamma_{xy0}\}^T$ are the incremental in-plane strains at the mid-surface of the section and $\Delta\{\kappa\} = \Delta\{\kappa_x, \kappa_y, \kappa_{xy}\}^T$ are the incremental curvatures. The incremental in-plane strains at a distance z from the mid-surface of the shell section become

$$\Delta\{\varepsilon\} = \Delta\{\varepsilon_0\} + z\Delta\{\kappa\} \tag{16}$$

Let h be the total thickness of the shell section, the incremental stress resultants, $\Delta\{N\} = \Delta\{N_x, N_y, N_{xy}\}^T$, $\Delta\{M\} = \Delta\{M_x, M_y, M_{xy}\}^T$ and $\Delta\{V\} = \Delta\{V_x, V_y\}$, can be defined as

$$\begin{Bmatrix} \Delta\{N\} \\ \Delta\{M\} \\ \Delta\{V\} \end{Bmatrix} = \int_{-h/2}^{h/2} \begin{Bmatrix} \Delta\{\sigma\} \\ z\Delta\{\sigma\} \\ \Delta\{\tau_t\} \end{Bmatrix} dz = \int_{-h/2}^{h/2} \begin{Bmatrix} [Q_1](\Delta\{\varepsilon_0\} + z\Delta\{\kappa\}) \\ z[Q_1](\Delta\{\varepsilon_0\} + z\Delta\{\kappa\}) \\ [Q_2]\Delta\{\gamma_t\} \end{Bmatrix} dz$$

$$= \int_{-h/2}^{h/2} \begin{bmatrix} [Q_1] & z[Q_1] & [0] \\ z[Q_1] & z^2[Q_1] & [0] \\ [0]^T & [0]^T & [Q_2] \end{bmatrix} \begin{Bmatrix} \Delta\{\varepsilon_0\} \\ \Delta\{\kappa\} \\ \Delta\{\gamma_t\} \end{Bmatrix} dz \tag{17}$$

where [0] is a 3-by-2 matrix with all the coefficients equal to zero.

For the nonlinear material case, the $[Q_1']$ matrix in Eq. (12) can be taken from Eqs. (6), (8) or (9) and the incremental stress resultants of Eq. (17) can be obtained by a numerical integration through the thickness of the composite shell section. For the linear material case, the $[Q_1']$ matrix used in Eq. (12) is taken from Eq. (3) and the incremental stress resultants of the shell section can be

written as a summation of integrals over the n laminae in the following form:

$$\begin{Bmatrix} \Delta\{N\} \\ \Delta\{M\} \\ \Delta\{V\} \end{Bmatrix} = \left(\sum_{j=1}^{n} \begin{bmatrix} (z_{jt} - z_{jb})[Q_1] & \frac{1}{2}(z_{jt}^2 - z_{jb}^2)[Q_1] & [0] \\ \frac{1}{2}(z_{jt}^2 - z_{jb}^2)[Q_1] & \frac{1}{3}(z_{jt}^3 - z_{jb}^3)[Q_1] & [0] \\ [0]^T & [0]^T & (z_{jt} - z_{jb})[Q_2] \end{bmatrix} \right) \begin{Bmatrix} \Delta\{\varepsilon_0\} \\ \Delta\{\kappa\} \\ \Delta\{\gamma_t\} \end{Bmatrix} \tag{18}$$

where z_{jt} and z_{jb} are distances from the mid-surface of the section to the top and the bottom of the jth layer, respectively.

5. Nonlinear finite element analysis

In the ABAQUS finite element program, the nonlinear response of a structure is modeled by an updated Lagrangian formulation and a modified Riks nonlinear incremental algorithm [19] can be used to construct the equilibrium solution path. To model bifurcation from the prebuckling path to the postbuckling path, geometric imperfections of composite plates are introduced by superimposing a small fraction (say 0.001 of the plate thickness) of the lowest eigenmode determined by a linearized buckling analysis to the original nodal coordinates of plates.

6. Numerical analyses

6.1. Composite plates with $[90/0]_{2S}$ and $[45/-45]_{2S}$ layups

In this section, composite laminate square plates with two laminate layups, $[90/0]_{2S}$ and $[45/-45]_{2S}$, are analyzed. The thickness of each ply is 1.02 mm (0.04 in). Ply constitutive properties and plate geometry are given in Fig. 1. The linear and nonlinear in-plane shear stress–strain curves are shown in Fig. 2. Both plates are subjected to uniform uniaxial compressive loads in the

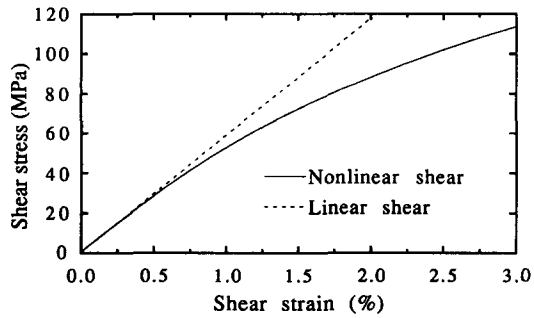

Fig. 2. In-plane shear stress–strain curves for composite lamina.

x direction. The edges of the plates are simply supported, which prevents out of plane motions but allows in-plane movements in x and y directions. In the numerical analysis, the entire plate is modeled by a 6×6 finite element mesh (36 shell elements).

To estimate the buckling loads and to generate geometric imperfections for composite plates, linearized buckling analyses are carried out first. The linearized buckling loads and buckling modes are shown in Fig. 3. The buckling modes of these two plates are very similar. Both plates buckle into a half-wave in the x direction and a half-wave in the y direction.

The load–displacement curves for the plate with a $[90/0]_{2S}$ layup are plotted in Fig. 4. The N_x is the total force (positive value means compression) applied to the edges and u_x is the associated end displacement (positive value means end extension and negative value means end shortening). It can be seen that the curves computed by using linear and nonlinear in-plane shear formulations are very close. Hence, nonlinear in-plane shear alone does not have much influence on the buckling and postbuckling responses of this plate. For the analysis carried out using the nonlinear in-plane shear formulation together with the Tsai–Wu criterion, the composite plate behaves almost linearly until a sudden collapse of the plate occurs. The predicted failure load is about 99% of the linearized buckling load.

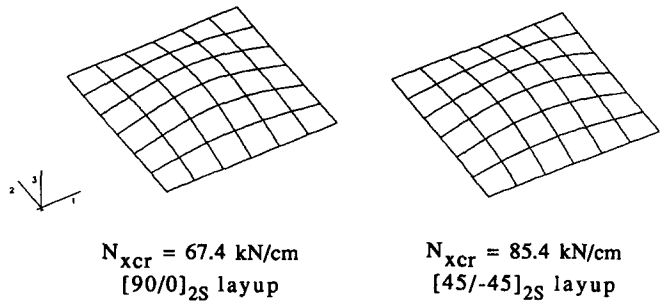

Fig. 3. Critical buckling loads and buckling modes for composite plates under uniaxial compression.

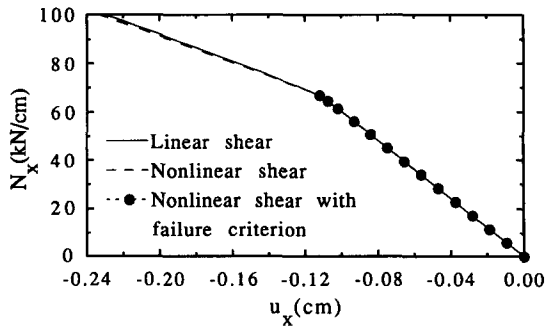

Fig. 4. Load–displacement curves for composite plate with $[90/0]_{2S}$ layup under uniaxial compression.

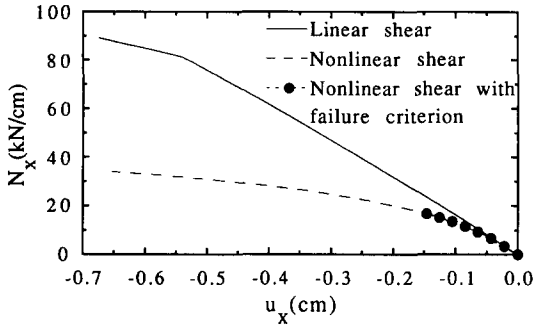

Fig. 5. Load–displacement curves for composite plate with $[45/-45]_{2S}$ layup under uniaxial compression.

Fig. 5 plots the load–displacement curves for the plate with a $[45/-45]_{2S}$ layup. With this kind of laminate layup, each lamina in the composite plate is subjected to severe shear loading. Therefore, it is a good sample to test the influence of nonlinear in-plane shear and failure theory on the buckling behavior of the plate. On contrary to the previous case, with the nonlinear in-plane shear formulation alone, the plate exhibits very nonlinear behavior throughout the entire loading stage. The load carrying capacity for the plate with the nonlinear in-plane shear formulation is much less than that with the linear shear formulation. For the analysis carried out using the nonlinear in-plane shear formulation together with the Tsai–Wu criterion, this plate exhibits a sudden failure mode while the loading is very low. The predicted failure strength of the composite plate is only about 19% of the linearized buckling load.

6.2. *Composite plates with* $[\pm\theta/90/0]_S$ *layups*

In this section, the $[\pm\theta/90/0]_S$ composite laminate plates are analyzed. The geometric and material properties, loading and finite element mesh of the plates are the same as those in the previous section.

Figs. 6–12 show the load–displacements curves, computed using the nonlinear in-plane shear formulation together with the Tsai–Wu criterion, for composite plates with various θ angles. For plates with θ equal to 0°, 30°, 60° and 90° (i.e., Figs. 6, 8, 10 and 12) additional load–displacement curves computed using the linear and nonlinear in-plane shear formulation are also plotted.

From Figs. 6, 8, 10 and 12, one can see that nonlinear in-plane shear alone does not have much influence on the buckling and postbuckling responses of these plates. For the analysis carried out using the nonlinear in-plane shear formulation together with the Tsai–Wu criterion, the composite plates with θ between 0° and 20° (Figs. 6 and 7) and with θ close to 90° (Fig. 12) behave almost linearly until a sudden collapse of the plates occur. For the other plates with θ between 30° and 80° (Figs. 8–11), they exhibit progressive failure mechanisms after the ultimate strengths of the plates have been reached.

In Fig. 13 the predicted ultimate strengths of the composite plates using the nonlinear shear formulation together with the Tsai–Wu criterion are compared with those obtained by the

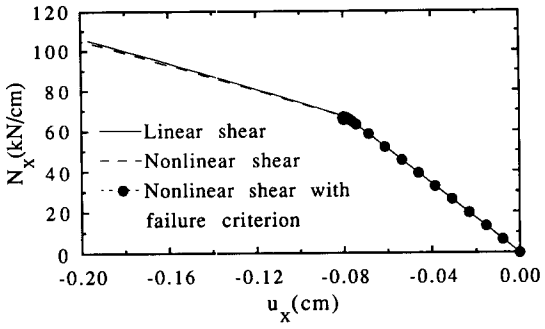

Fig. 6. Load–displacement curves for composite plate with $[\pm 0/90/0]_S$ layup under uniaxial compression.

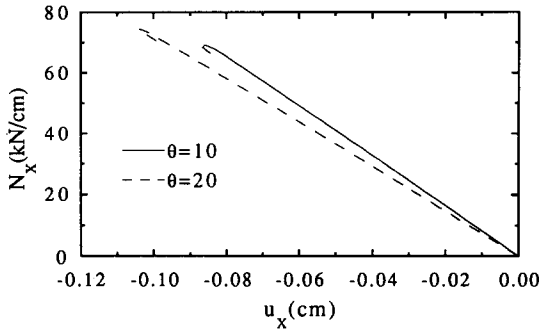

Fig. 7. Load–displacement curves for composite plates with $[\pm 10/90/0]_S$and $[\pm 20/90/0]_S$ layups under uniaxial compression (nonlinear shear with failure criterion only).

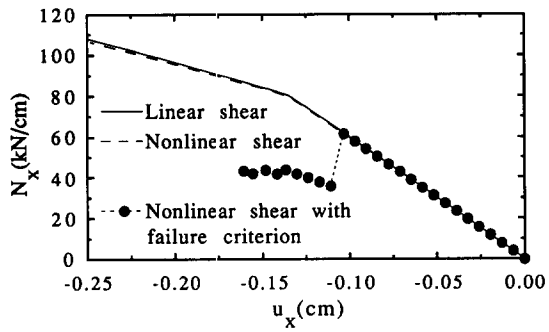

Fig. 8. Load–displacement curves for composite plate with $[\pm 30/90/0]_S$ layup under uniaxial compression.

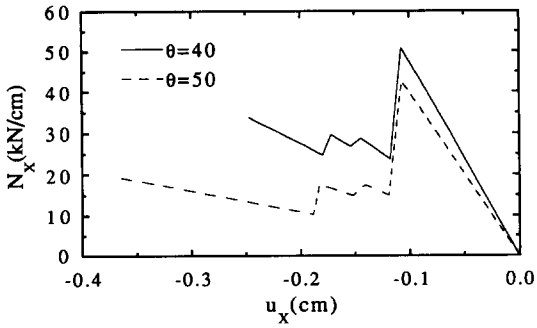

Fig. 9. Load–displacement curves for composite plates with $[\pm 40/90/0]_S$ and $[\pm 50/90/0]_S$ layups under uniaxial compression (nonlinear shear with failure criterion only).

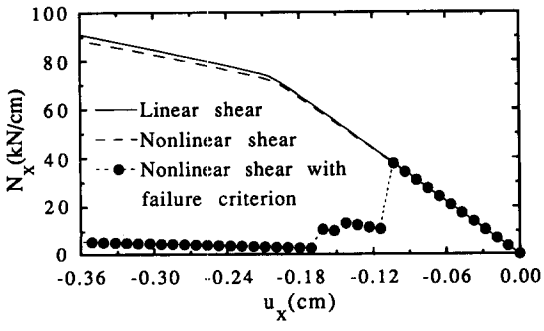

Fig. 10. Load–displacement curves for composite plate with $[\pm 60/90/0]_S$ layup under uniaxial compression.

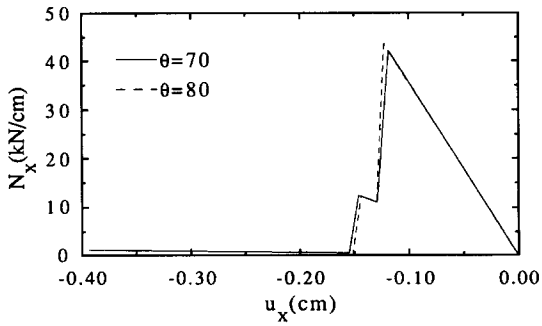

Fig. 11. Load–displacement curves for composite plates with $[\pm 70/90/0]_S$ and $[\pm 80/90/0]_S$ layups under uniaxial compression (nonlinear shear with failure criterion only).

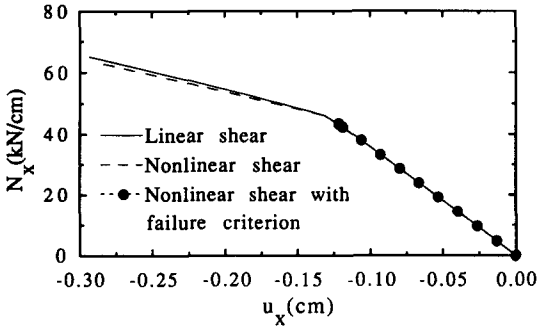

Fig. 12. Load–displacement curves for composite plate with $[\pm 90/90/0]_S$ layup under uniaxial compression.

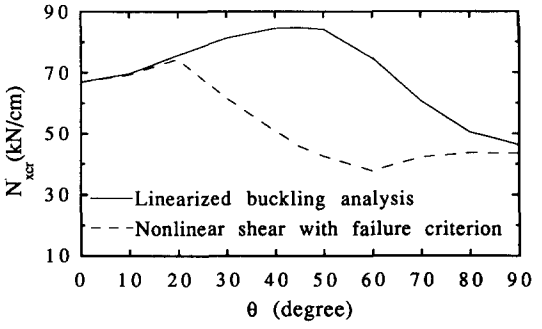

Fig. 13. Critical load N_{xcr} as a function of θ for composite plate with $[\pm\theta/90/0]_S$ layup under uniaxial compression.

linearized buckling analyses. From this figure, one can see that the predicted ultimate strengths of the plates with θ between 0° and 20° and with θ close to 90° are very close to the linearized buckling loads. On the other hand the predicted ultimate strengths of the plates with θ between 30° and 80° are much lower than the linearized buckling loads. It can also be observed that the optimal fiber angle θ for the plates with the material nonlinear analysis seems around 20°. This is quite different from the optimal fiber angle for the plates with linearized buckling analysis, which seems between 40° and 50°.

7. Conclusions

For the material nonlinear analysis of composite plates with various laminate layups, the following conclusions can be drawn.

1. The nonlinear in-plane shear alone does not have much influence on the buckling responses and buckling strengths of the plates with $[90/0]_{2S}$ and $[\pm\theta/90/0]_S$ layups.

2. The nonlinear in-plane shear together with material failure according to the Tsai–Wu theory has great influence on the buckling and postbuckling responses of the plates with $[90/0]_{2S}$ and $[\pm\theta/90/0]_S$ layups. Its effect on the reduction of ultimate strengths and postbuckling stiffness of these plates depends on the laminate layups.

3. The nonlinear in-plane shear alone has significant influence on the buckling response of the plate with a $[45/-45]_{2S}$ layup. In addition, if the Tsai–Wu criterion is considered, the plate exhibits a sudden failure mode and the predicted ultimate strength of the composite plate is much lower than the linearized buckling load.

4. The optimal fiber angle θ for the $[\pm\theta/90/0]_S$ composite plates with the analysis using the nonlinear in-plane shear formulation and the Tsai–Wu failure theory is quite different from that obtained using the linearized buckling analysis.

Acknowledgement

The author wishes to express his appreciation to Dr. Su Su Wang, the Distinguished University Professor of the University of Houston, TX, USA, for his fruitful discussion during the early stage of this study.

References

[1] A.W. Leissa, Buckling of laminated plates and shell panels, AFWAL-TR-85-3069 Air Force Wright Aeronautical Laboratories, Wright-Patterson Air Force Base, OH, 1985.
[2] S.P. Engelstad, J.N. Reddy and N.F. Knight, "Postbuckling response and failure prediction of flat rectangular graphite-epoxy plates loaded in axial compression", *Proc. of the 32th AIAA/ASME/ASCE/AHS/ASC Structures, Structural Dynamics and Materials Conf.*, AIAA, Washington, DC, pp. 888–895, 1991.
[3] A.K. Noor, J.H. Starnes and W.A. Waters, 'Postbuckling response simulations of laminated anisotropy panels", *J. Aerospace Eng.* **5**, pp. 347–368, 1992.
[4] L. Librescu and M. Stein, "Postbuckling of shear deferrable composite flat panels taking into account geometrical imperfections", *AIAA J.* **30**, pp. 1352–1360, 1992.
[5] H.T. Hahn and S.W. Tsai, "Nonlinear elastic behavior of unidirectional composite laminae", *J. Compos. Mater.* **7**, pp. 102–118, 1973.
[6] R.M. Jones and H.S. Morgan, "Analysis of nonlinear stress–strain behavior of fiber-reinforced composite materials", *AIAA J.* **15**, pp. 1669–1676, 1977.
[7] Z. Hashin, D. Bagchi and B.W. Rosen, Nonlinear behavior of fiber composite laminates, NASA Contractor Report, NASA CR-2313, 1974.
[8] R. Hajali and S.S. Wang, Nonlinear behavior of fiber composite materials and its effect on the postbuckling response of laminated plates, UIUC-NCCMR-90-10, National Center for Composite Materials Research, University of Illinois, Urbana, IL, 1990.
[9] R.R. Arnold and J. Mayers, "Buckling, postbuckling, and crippling of materially nonlinear laminated composite plates", *Int. J. Solids Struct.* **20**, pp. 863–880, 1984.
[10] C.T. Sun and J.L. Chen, "A simple flow rule for characterizing nonlinear behavior of fiber composites", *J. Compos. Mater.* **23**, pp. 1009–1020, 1989.
[11] R. Vaziri, M.D. Olson and D.L. Anderson, "A plasticity-based constitutive model for fibre-reinforced composite laminates", *J. Compos. Mater.* **25**, pp. 512–535, 1991.
[12] A. Nanda and T. Kuppusamy, "Three-dimensional elastic-plastic analysis of laminated composite plates", *Compos. Struct.* **17**, pp. 213–225, 1991.
[13] R.E. Rowlands, "Strength (failure) theories and their experimental correlation", in: G.C. Sih and A.M. Skudra (eds.), *Failure Mechanics of Composites*, Elsevier, Amsterdam, pp. 71–125, 1985.
[14] Hibbitt, Karlsson and Sorensen, Inc., *ABAQUS Theory Manual and User Manual*, Version 4-9, Providence, RI, 1992.
[15] R.D. Mindlin, "Influence of rotatory inertia and shear on flexural motions of isotropic elastic plates", *J. Appl. Mech.* **18**, pp. 31–38, 1951.
[16] S.W. Tsai and E.M. Wu, "A general theory of strength for anisotropic materials", *J. Compos. Mater.* **5**, pp. 58–80, 1971.
[17] R. Narayanaswami and H.M. Adelman, "Evaluation of the tensor polynomial and Hoffman strength theories for composite materials", *J. Compos. Mater.* **11**, pp. 366–377, 1977.
[18] B.M. Irons, "The semi-loof shell element" in: D.G. Ashwell and R.H. Gallagher (eds.), *Finite Elements for Thin Shells and Curved Members*, Wiley, London, pp. 197–222, 1976.
[19] E. Riks, "An incremental approach to the solution of snapping and buckling problems", *Int. J. Solids Struct.* **15**, pp. 529–551, 1979.